

THE EFFECT OF COPPER ADDITION ON MICROSTRUCTURAL AND WEAR PROPORTION OF ALUMINIUM BASED METALPOWDER COMPOSITIES

Satendra kumar¹; Tribhuwan kishore Mishra²; Vivek Gedam³

¹M.Tech Scholar, "Gyan Ganga Institute of Technology and Sciences, Jabalpur (M.P.)"

^{2&3}Assistant Professor, "Gyan Ganga Institute of Technology and Sciences, Jabalpur (M.P.)"

ABSTRACT

In this paper we are proposing the method of investigating the effect of copper addition on microstructure of aluminium based metal powder composities. In the reference powder metallurgy is the key process of obtaining metal powder composities. Base metal powders used are of aluminium, copper powder, we include graphite for lubrication as Tungsten Carbide powder. Obtained samples were induced to various destructive and non destructive tests, hence forth the results obtained are compared which provided us the final conclusion related to the copper addition effect.

Key words: microstructure, powder metallurgy, metal powder composities, destructive tests, non destructive tests

1. INTRODUCTION

Powder metallurgy

Powder metallurgy is used to make unique materials with tailored properties, impossible to achieve from melting or forming with other methods. It enables combinations of materials that would otherwise be impossible to mix and processing of materials with very high melting points, in our process of project we have used a standardized powder metallurgy method, as defined in figure 1.1 below:

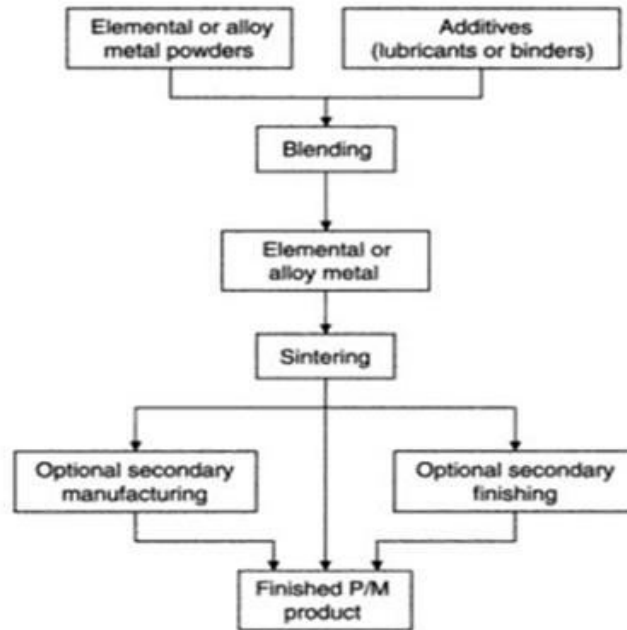


Fig 1.1: Various steps involved in Powder Metallurgy

2. Wear mechanism

Wear is the material removal process by metal to metal contact, metal to abrasive practical contact, or metal to erosive practical. The definition of wear may include loss of dimension from plastic deformation if it is the result of mechanical action at the interface between two surfaces.

There are three stages of wear under normal loads and practical conditions.

- a) Primary or early run-in-period stage- When surfaces come in contact with each other, wear rate starts to vary from low wear to high wear rate.
- b) Secondary or mid-age process wear- In this stage, steady rate wear takes place. The operational life of components is included in this stage.
- c) Tertiary stage or old age period wear- Failure of components occurs in this stage due to a higher rate of wear.

Some commonly referred to wear mechanisms (or processes) include:

Adhesive wear; Abrasive wear; Surface fatigue; Fretting wear; Erosive wear

3. METHODOLOGY

The various processes which are involved in completion of project are being defined in the present flow chart

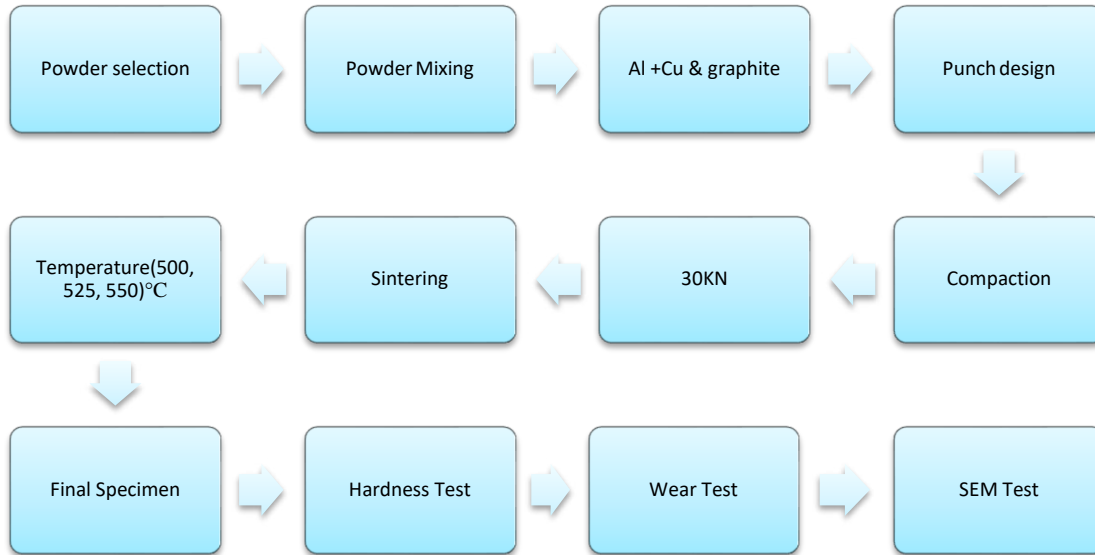


Figure3.1: Flow Chart of Experiments

4. Material Procurement:

The Aluminium powder, Copper powder, Tungsten carbide and the graphite powder purchased from Qualikems Fine Chemicals Pvt. Ltd., Vadodara. Specification of Aluminium, copper, and Graphite powder are as follows-

Aluminium Powder Specification: Electrolytic Aluminum powder of purity 99.7% was used throughout the experiments.

Table 4.1: Aluminium Powder Specification

Element	Al ≥	Fe	Si	Cu	Mn	Zn	H
Wt%	99.7	0.17	0.1313	0.0015	0.023	0.0053	0.04879

Copper Powder Specification: Atomized Tungsten carbide powder of purity 99.5%.

Table 4.2 Copper Powder Specifications

Element	Cu ≥	Sb	As	Pb	Fe	Mn	Ag	Sn
wt. %	99.5	0.005	0.002	0.5	0.005	0.005	0.005	0.005

Graphite for lubrication Specification: Electrolytic Tungsten Carbide powder of purity 98.2%.

Table 4.3 Graphite Powder Specification

Element	WC	Ni	Fe	Cr	Mo	O
wt. %	98.2	0.3	0.5	0.1	0.1	0.8

Die & Punch Preparation

In order to manufacture the specimen pins of the Copper-Tungsten carbide powder preforms a die and punch has been manufactured by turning the die steel on lathe.

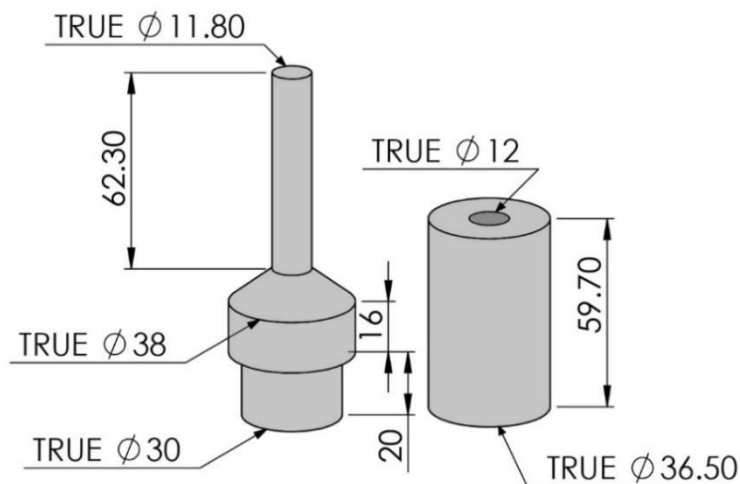


Figure 4.1: Die and Punch

Design of Experiment

- **Selection of sintering temperature:** this sintering temperature was used for this work: $T = 550^{\circ}\text{C}$
- **Selection of Copper content (weight percentage):** $\text{Cu}_1 = 0$; $\text{Cu}_2 = 4$; $\text{Cu}_3 = 8$; $\text{Cu}_4 = 12$
- **Selection of sample:** In this investigation 12 samples were prepared with different combinations of sintering temperature and Copper content.

Process of Experiment

Aluminium, Tungsten carbide powders were mixed in varying compositions of Copper powder. The percentage of copper was varied with different weight percentages. The different percentages of copper are 0%, 4%, 8%, 12%, and 5% tungsten Carbide as graphite for lubrication is used in all samples.

Then, the samples were taken and blended together properly by manual mixing for 15 minutes to ensure uniform distribution of the Tungsten carbide and copper particles throughout the Aluminium matrix.

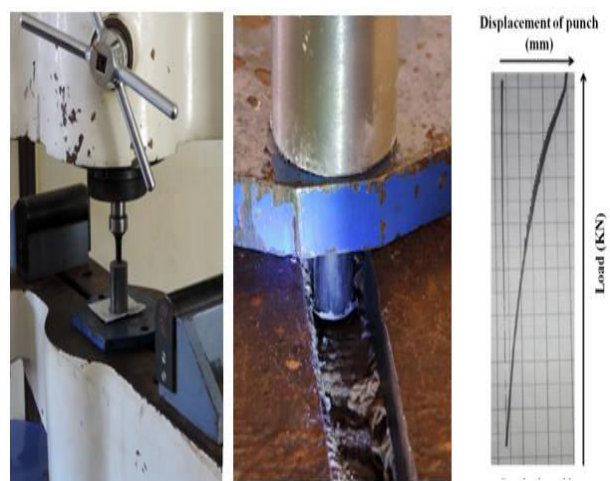
Cold Compaction Process

The most common way of compacting is axial pressing in a steel die under pressure. It is possible to press parts with complicated shapes in a single operation and with a high production rate. The part achieves sufficient strength to be ejected from the tool die. The blended samples were then cold compacted by applying a uni-axial press of 30KN in a die of 12mm diameter. For powder compaction, UTM machine is used (compaction procedure should done very slow feed rate for uniform compaction without any damage in punch and sample) When punch goes downward direction air bubble exerted from powder mixture in die and retract the punch in the upward direction, this prevents load sound of penetration.

Fig 4.2 Universal Testing Machine



Fig4.3: Cold compaction and UTM plotted graph



Sintering Process

Sintering of the green compacts is then being carried out in a muffle furnace shown in the figure below. This furnace is being provided with the controller cum programmer that can be programmed the sintering time and the soaking time. The sintering process is being performed in an endothermic atmosphere. The arrangement of crucibles containing a sand and the green compact is being shown in Figure 4.4.



Figure 4.4: Chronological order of sintering arrangements

Table 4.4: Sintering parameters

S.no.	Sintering Temperature °C	Time to reach Sintering temperature. (Min.)	Still temperature time (min.)
1	550	60	30

The following graphs shows variation of sintering cycle in terms of temperature and time comparison graph.

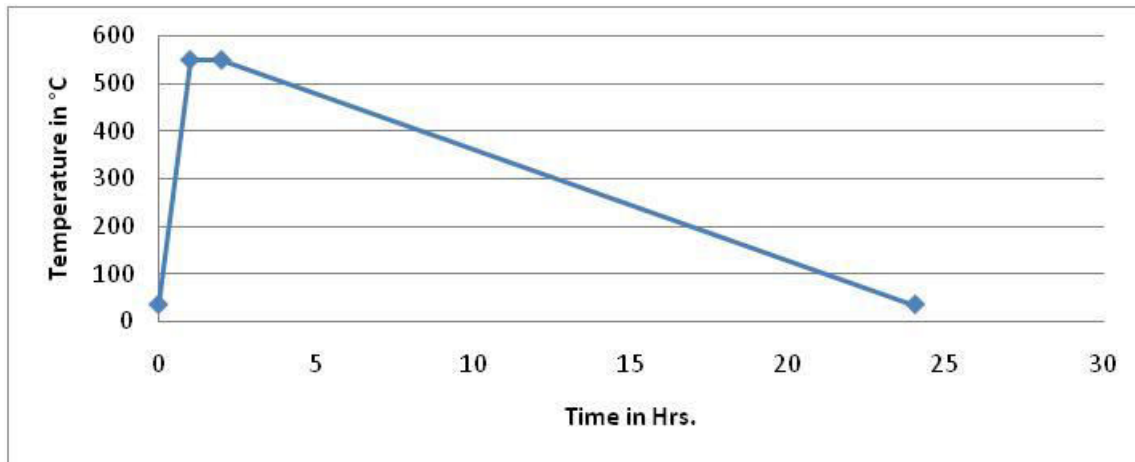


Figure 4.5: Sintering Cycle for 550°C

Abrasive Wear

Two body abrasive wear tests were conducted using the pin on disk tester (TA-200LE, Magunun Engineers, Bangalore, India). Silicon carbide abrasive media of 400 μm sized with angular shape was mounted on a circular disc of diameter 165 mm. The weight-loss method was used to measure the wear at 500 m, 1000m, and 1500 m sliding distance. Pin sample was pressed against silicon carbide abrasive media as a counter body. After every 500 m sliding distance, the abrasive paper was replaced to retain accurate contact between the pin specimen and the abrasive medium.

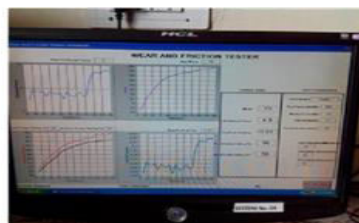


Figure 4.6: Wear Tester Machine

5. RESULTS

SEM Analysis of sample

In this section, the microscopic structure of manufactured specimens taken by Scanning Electron Microscope has been analyzed. An analysis is done to find the study the structure formed after sintering.

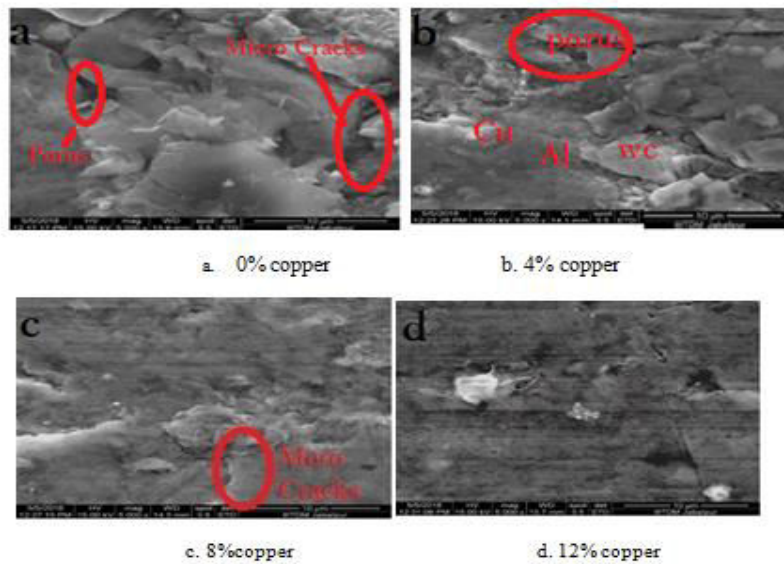


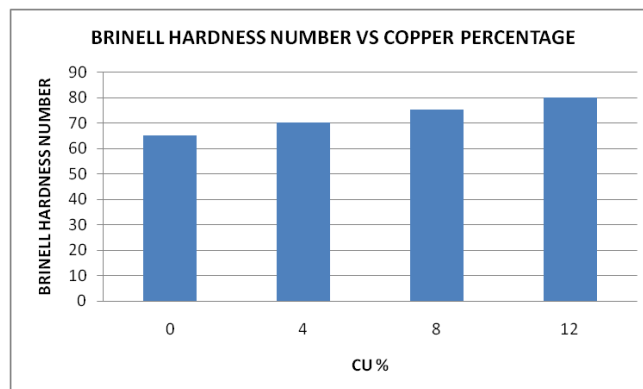
Figure 5.1: SEM results for Different Specimen

(a.0% Copper, b. 4% Copper, c. 8% Copper, d. 12% Copper)

Effect of Cu% and Sintering Temperature on Hardness

The effect of Cu content and sintering temperature on hardness is being described in present graph. The increased hardness is attributed to the copper particles, which act as barriers and prevent the movement of dislocations within the matrix. It was found that as Cu% increases, hardness is also increased because the copper increases density. It is verified by microstructure. As the sintering temperature increases, the hardness shows an increasing trend because bounding increases with temperature.

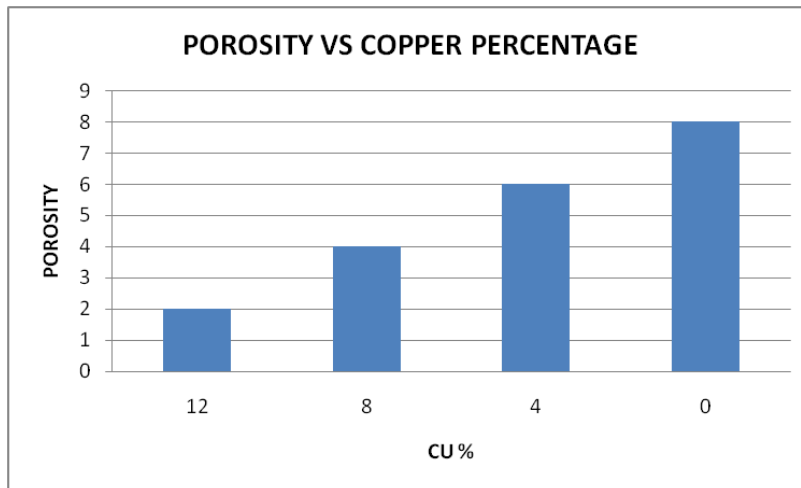
Figure 5.2: Effect of Copper Percentage on Brinell Hardness Number



Effect of Cu% and Sintering Temperature on Porosity

The variation of porosity with respect to Cu (wt %) and sintering temperature. It was found that as Cu contents increases, density shows a decreasing trend. Sample at 0 (wt %) shows maximum density various sample at 12 (wt %) Cu shows the minimum density. Yet sintering temperature is kept constant at 550⁰C.Porous have been migrating from boundaries into the interior grain.

Figure 5.3: Effect of Copper Percentage on Porosity



Abrasive wear with respect to Copper percentage

Experimental results clearly shows the variation of abrasive wear with respect to copper percentage, at 0 % copper value of abrasive wear is highest i.e 111% and at 12% copper it is lowest i.e 0 %, similarly the values of abrasive wear varies in context to other copper percentages as for 4% Cu it gives value of 78% and for 8% Cu it gives value of 33%, hence the comparison shows that 0% Cu gives us more good abrasive value.

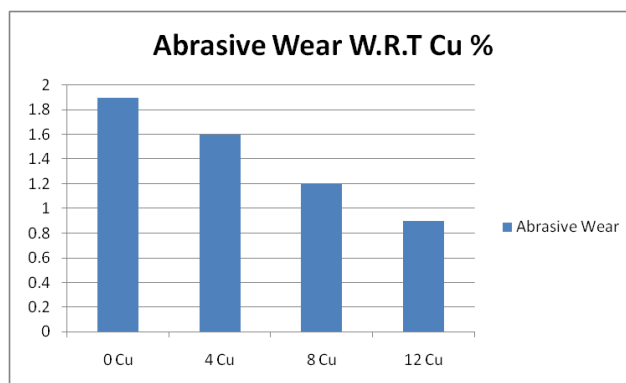


Figure 5.4: Abrasive Wear Variation with respect to Cu %

COF Variation With Respect To Time

Coefficient of friction variation with time graph shows that, 0% copper content sample as compared to others has low value of COF, where as highest percentage of copper content that is 12%, shows highest value of COF. Overall comparison shows that as we increase the copper percentage value of coefficient of friction value is also increasing with that.

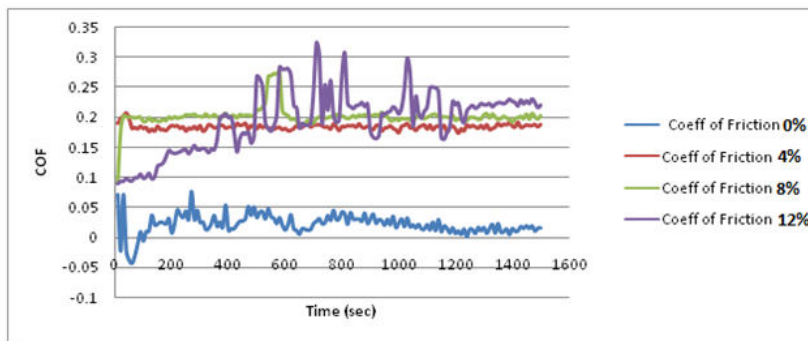


Figure 5.5: COF Variation with respect to Time

6. CONCLUSION

From the experiment result in analysis following conclusions were finding out of Al-Cu Metal powder composite.

The addition of Cu refines the microstructure due to strong bonding between Al and Cu particles. The Al and Cu sintered specimen exhibits dense microstructure when Cu is increased up to optimum addition of 12 wt. % the extra amount of Cu flout on the upper surface and increases the hardness of the the prepared specimen.

XRD results also confirms the presence of various major and minor phases of Al-Cu, which increases the hardness of the matrix.

Hardness increases of sintered specimen up to optimum addition of 12 wt. % of Cu. Al-0 wt.% Cu, Al-4 wt.% Cu, Al-8 wt.% Cu, and Al-12 wt. % Cu exhibit hardness in 65, 70, 74 and 80 BHN, respectively. The higher hardness of the Al-12 wt. % Cu sintered specimen can be attributed to refining and dense microstructure.

Porosity decreases of sintered specimen up to optimum addition of 12 wt. % of Cu. Al-0 wt.% Cu, Al-4 wt.% Cu, Al-8 wt.% Cu, and Al-12 wt. % Cu exhibit hardness in 7.5, 5.9, 3.8 and 1.7 respectively. The highest value of porosity we obtain at Al-0 wt. % Cu sintered specimen.

Al-12 wt. % Cu specimen shows higher wear loss, and Al-0 wt. % Cu, sintered specimen exhibits minimum wear, Al-4 wt.% Cu, Al-8 wt.% Cu, and Al-12 wt. % Cu sintered samples shoes 1.4, 1.5 and 1.8 higher wear loss as compared to Al-0 wt.% Cu.

The addition of tungsten Carbide increases the COF, and Al-12 wt. % Cu specimen shows a higher coefficient of friction, whereas Al-0 wt.% Cu shows a minimum coefficient of friction.

Cutting, ploughing, and fracture wear mechanisms were identified in the sintered specimen. Small grooves were seen in Al-8 wt.% Cu, and deep grooves were seen in the Al-12 wt. % Cu worn-out surface of the sintered sample.

7. REFERENCES

- Shaik, M.A.; Golla, B.R. Two body abrasion wear behaviour of Cu-ZrB₂ composites against SiC emery paper. *Wear* **2020**, *450*, 450–451.
- Guiderdoni, C.; Estournès, C.; Peigney, A.; Weibel, A.; Turq, V.; Laurent, C. The preparation of double-walled carbon nanotube/Cu composites by spark plasma sintering, and their hardness and friction properties. *Carbon* **2011**, *49*, 4535–4543.
- Rabinarayan, S.; Kumar, O.R. Study of Dry-Sliding Wear Behaviour of Cu-SiCp Metal Matrix Composites. *Mater. Today Proc.* **2020**, *21*, 1255–1259.
- Zhao, H.; Feng, Y.; Qian, G.; Huang, X.; Guo, S.; Sun, X. Effect of Ti₃AlC₂ Content on Electrical Friction and Wear Behaviors of Cu-Ti₃AlC₂ Composites. *Tribol. Lett.* **2019**, *67*, 96.
- .
- Li, X.; Wei, S.; Yang, Q.; Gao, Y.; Zhong, Z. Tribological performance of self-matching pairs of B₄C/hBN composite ceramics under different frictional loads. *Ceram. Int.* **2020**, *46*, 996–1001.
- Li, X.; Gao, Y.; Yang, Q. Sliding tribological performance of B₄C-hBN composite ceramics against AISI 321 steel under distilled water condition. *Ceram. Int.* **2017**, *43*, 14932–14937.
- Li, X.; Gao, Y.; Wei, S.; Yang, Q.; Zhong, Z. Dry sliding tribological properties of self-mated couples of B₄C-hBN ceramic composites. *Ceram. Int.* **2017**, *43*, 162–166.
- Li, X.; Gao, Y.; Wei, S.; Yang, Q. Tribological behaviors of B₄C-hBN ceramic composites used as pins or discs coupled with B₄C ceramic under dry sliding condition. *Ceram. Int.* **2017**, *43*, 1578–1583. *Metals* **2021**, *11*, 1250 13 of 13

- Li, X.; Gao, Y.; Song, L.; Yang, Q.; Wei, S.; You, L.; Zhou, Y.; Zhang, G.; Xu, L.; Yang, B. Influences of hBN content and test mode on dry sliding tribological characteristics of B4C-hBN ceramics against bearing steel. *Ceram. Int.* **2018**, *44*, 6443–6450.
- Lyu, Y.; Sun, Y.; Jing, F. On the microstructure and wear resistance of Fe-based composite coatings processed by plasma cladding with B4C injection. *Ceram. Int.* **2015**, *41*, 10934–10939.
- Celik, Y.H.; Kilickap, E. Hardness and Wear Behaviours of Al Matrix Composites and Hybrid Composites Reinforced with B4C and SiC. *Powder Metall. Met. Ceram.* **2019**, *57*, 613–622.
- Joshi, S.; Yuvaraj, N.; Singh, R.C.; Chaudhary, R. Microstructural and Wear Investigations of the Mg/B4C Surface Composite Prepared Through Friction Stir Processing. *Trans. Indian Inst. Met.* **2020**, *73*, 3007–3018.
- Pandey, S.; Shrivastava, P.K. Vibration-assisted electrical arc machining of 10% B4C/Al metal matrix composite. *Proc. Inst. Mech. Eng. Part C J. Mech. Eng. Sci.* **2019**, *234*, 1156–1170.
- Namini, A.S.; Delbari, S.A.; Nayebi, B.; Asl, M.S.; Parvizi, S. Effect of B4C content on sintering behavior, microstructure and mechanical properties of Ti-based composites fabricated via spark plasma sintering. *Mater. Chem. Phys.* **2020**, *251*, 123087.
- Hynes, N.R.J.; Raja, S.; Tharmaraj, R.; Pruncu, C.I.; Dispinar, D. Mechanical and tribological characteristics of boron carbide reinforcement of AA6061 matrix composite. *J. Braz. Soc. Mech. Sci. Eng.* **2020**, *42*, 155.
- Aherwar, A.; Patnaik, A.; Pruncu, C.I. Effect of B4C and waste porcelain ceramic particulate reinforcements on mechanical and tribological characteristics of high strength AA7075 based hybrid composite. *J. Mater. Res. Technol.* **2020**, *9*, 9882–9894.
- Prajapati, P.K.; Chaira, D. Fabrication and Characterization of Cu–B4C Metal Matrix Composite by Powder Metallurgy: Effect of B4C on Microstructure, Mechanical Properties and Electrical Conductivity. *Trans. Indian Inst. Met.* **2019**, *72*, 673–684.
- Balalan, Z.; Gulan, F. Microstructure and mechanical properties of Cu-B4C and CuAl-B4C composites produced by hot pressing. *Rare Met.* **2019**, *38*, 1169–1177.
- Qin, Q.; Wang, T.; Hua, J. Effect of B4C Content on Friction and Wear Properties of Copper-based Powder Metallurgy Friction Materials. *Lubr. Eng.* **2017**, *42*, 77–81.
- Bai, H. Preparation and Research of Diamond (Boron Carbide)/Metal Composite Encapsulation Material. Ph.D. Thesis, Huazhong University of Science and Technology, Wuhan, China, 2013.